JOURNAL OF MAGNETIC RESONANCE IMAGING 12:645–649 (2000)

Technical Note

Accurate Localization of Needle Entry Point in Interventional MRI

V. Daanen, MS,[1,2] E. Coste, PhD,[1] G. Sergent, MD,[3] F. Godart, MD,[4] C. Vasseur, PhD,[2] and J. Rousseau, PhD[1]*

In interventional magnetic resonance imaging (MRI), the systems designed to help the surgeon during biopsy must provide accurate knowledge of the positions of the target and also the entry point of the needle on the skin of the patient. In some cases, this needle entry point can be outside the B_0 homogeneity area, where the distortions may be larger than a few millimeters. In that case, major correction for geometric deformation must be performed. Moreover, the use of markers to highlight the needle entry point is inaccurate. The aim of this study was to establish a three-dimensional coordinate correction according to the position of the entry point of the needle. We also describe a 2-degree of freedom electromechanical device that is used to determine the needle entry point on the patient's skin with a laser spot. J. Magn. Reson. Imaging 2000;12:645–649. © 2000 Wiley-Liss, Inc.

Index terms: interventional MRI; needle entry point; geometrical distortions; MR-guided biopsy

DURING PLANNING OF MR-guided biopsy, puncture, or guide placement, the surgeon has to define the target point to be reached as well as the point of entry on the skin of the patient. These points are defined on images obtained from the MR scanner during the intervention. One generally locates this entry point by tomographic landmarks or manually by creating an artifact on the skin during image acquisition (Fig. 1). These methods present several disadvantages, particularly a) the need for roughly knowing the localization of the entry point; and b) localization inaccuracy relating to the size of the marker used.

Furthermore, whereas the target point is always inside the homogeneous area of the main magnetic field (B_0), the point of entry may be outside this homogeneity area, with large geometric distortions in the image (1). This results in three-dimensional (3D) coordinate inaccuracy and involves an error on the trajectory. We thus considered it necessary to ensure the reliability of the trajectory calculated from the positions of the target point and the entry point. When the entry point is outside the zone of homogeneity of B_0, we correct the coordinates of this point by a fast, accurate, and easy-to-use correction method. We then illuminate the entry point by a laser spot, monitored by an optical stereolocalization device, to indicate accurately the position of this point on the skin of the patient.

MATERIALS AND METHODS

All methods and measurements were carried out on an OPEN 0.2-T MR scanner (Siemens Medical Systems, Erlangen, Germany) equipped with resistive magnet and well designed for interventional MRI.

Correction of Geometric Deformations

Method of Correction

To evaluate the image distortions and to correct them, we designed a calibration phantom, which consists of 750 spherical balls (15 mm in diameter) arranged in a regular cubic pattern with 30-mm side length. The gross dimensions of the phantom were 400 × 300 × 210 mm (Fig 2a).

Images of the phantom were obtained in three planes, sagittal, axial, and coronal (Fig. 2b), using different multislice sequences. The images were processed to determine the center of mass of each ball within every image (Fig. 2c). These data were then three-dimensionally merged with a weighting factor depending on the image contrast (to avoid a displacement of the coordinates of the balls due to partial volume effect). Assuming that the image deformation is negligible at the center of the homogeneity area, the theoretical coordinates of each ball were determined in a reference trihedron whose center is located on the ball closest to the magnet isocenter.

The correction method we used is similar to that described to correct video images (2). We simply expanded this method to include 3D distortions.

[1]ITM, University Hospital, 59037 Lille, France.
[2]I3D, Sciences University, 59037 Lille, France.
[3]Radiology Department, University Hospital, 59037 Lille, France.
[4]Cardiology Department, University Hospital, 59037 Lille, France.

Contract grant sponsor: Direction de la Recherche et des Etudes Doctorales (DRED); Contract grant number: EA 1049; Contract grant sponsor: Centre Hospitalier Universitaire of Lille (CLARC); Contract grant number: 93.01; Contract grant sponsor: Ministère de la Santé Contract grant number: PHRC 1998; Contract grant sponsor: Ministère de l'Industrie; Contract grant number: ANRT, CIFRE 453/96.

Presented at the 7th Scientific Meeting and Exhibition of the ISMRM, Philadelphia, 1999.

*Address reprint requests to: J.R., Interventional MRI Group, ITM, Pavillon Vancostenobel, CHRU, 59037 Lille, France.
E-mail: jrousseau@ chru-lille.fr

Received March 2, 2000; Accepted July 6, 2000.

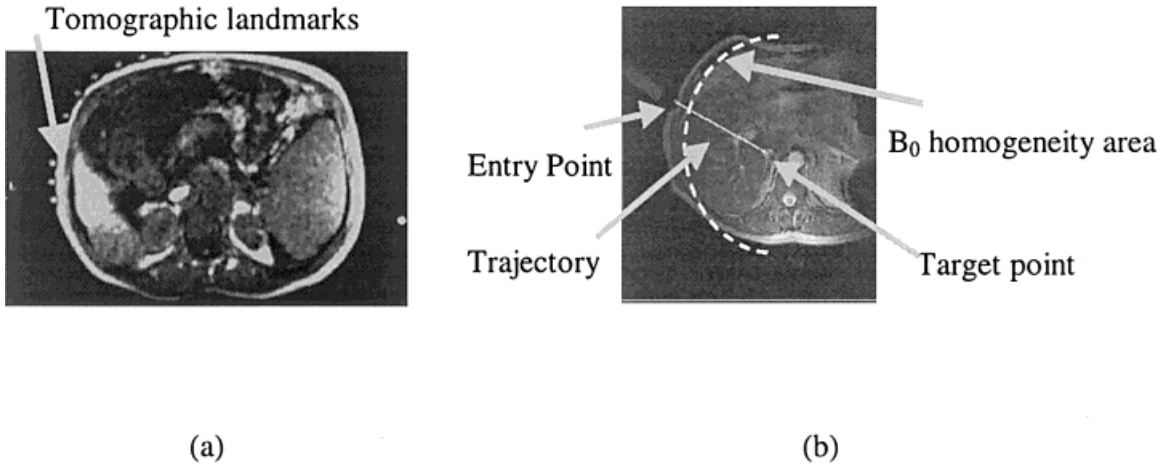

Figure 1. Trajectory determination in interventional MRI, **(a)** using tomographic landmarks and **(b)** using a local artifact on the patient's skin. The point of entry may be outside the B_0 homogeneity volume.

Let P be a point within the 3D distorted volume having coordinates (X_{Pm}, Y_{Pm}, Z_{Pm}). First, we localize the eight closest balls, Bi (I = 1–8), within the phantom. Let the measured positions of these balls be (X_{Bim}, Y_{Bim}, Z_{Bim}). Next, we determine the weighting factors Wi (I = 1–to 8) by using the well-known least squares fitting technique in such a manner that:

$$\begin{bmatrix} X_{Pm} \\ Y_{Pm} \\ Z_{Pm} \end{bmatrix} = \begin{bmatrix} X_{Bim} \ldots X_{B8m} \\ Y_{Bim} \ldots Y_{B8m} \\ Z_{Bim} \ldots Z_{B8m} \end{bmatrix} \begin{bmatrix} w_1 \\ \ldots \\ w_8 \end{bmatrix}$$

Under these conditions, the corrected coordinates of P (X_{Pc}, Y_{Pc}, Z_{Pc}) are given by:

$$\begin{bmatrix} X_{Pc} \\ Y_{Pc} \\ Z_{Pc} \end{bmatrix} = \begin{bmatrix} X_{Bic} \ldots X_{B8c} \\ Y_{Bic} \ldots Y_{B8c} \\ Z_{Bic} \ldots Z_{B8c} \end{bmatrix} \begin{bmatrix} w_1 \\ \ldots \\ w_8 \end{bmatrix}$$

where (X_{Bic}, Y_{Bic}, Z_{Bic}) are the corrected coordinates of the balls of the phantom.

Validation of the Method

To validate the method of correction, we built a test object composed of five markers localized on a plate with a 120-mm side (Fig. 3). In all the measurements, markers 1 and 2 are always localized inside the B_0 homogeneity area, whereas markers 3, 4, and 5 are positioned far from this area. The errors in distance between different markers, measured in the corrected images, were chosen to evaluate the accuracy of the method of correction.

Illumination of the Entry Point and Needle Guidance

To plan the intervention, the physician defines the point of entry on the MR images. To locate this point on the patient's skin, we designed a 2-degree of freedom electromechanical LASER pointing device (Fig. 4), which indicates the entry needle point on the skin with a red spot. It uses two-step motor reducers (60 steps/turns, reduction ratio 320), which ensures angular resolution of about 0.5 minute (ie, 0.5 mm resolution at a distance of 3 m). This pointer is controlled (displacement, on/off laser diode) by a host microcomputer, located outside the magnet room. Fiberoptic links to the pointer are used to avoid MR artifacts.

To ensure a high accuracy of indication, the laser spot is servo-controlled by a stereo-localization system consisting of four CCD cameras mounted in the MR

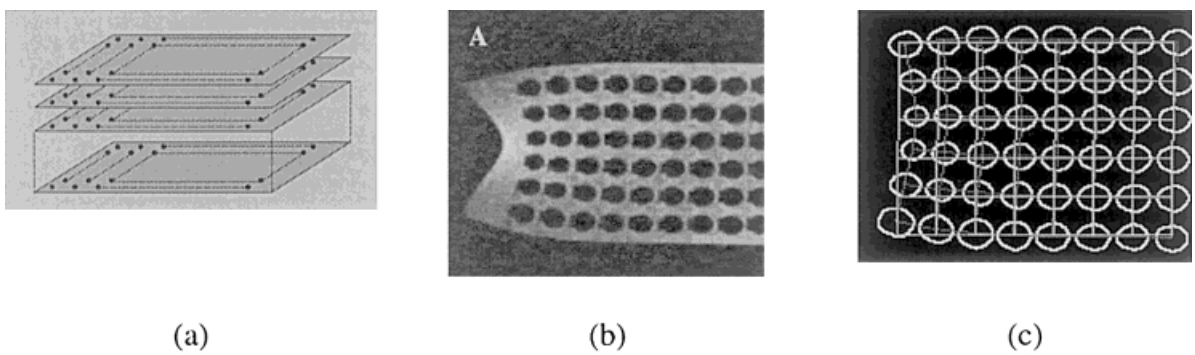

Figure 2. Calibration phantom. **a:** Regular cubic pattern: interplane distance is 30 mm. **b:** MR coronal image of the phantom. **c:** Center of mass determination of the balls in the previous image.

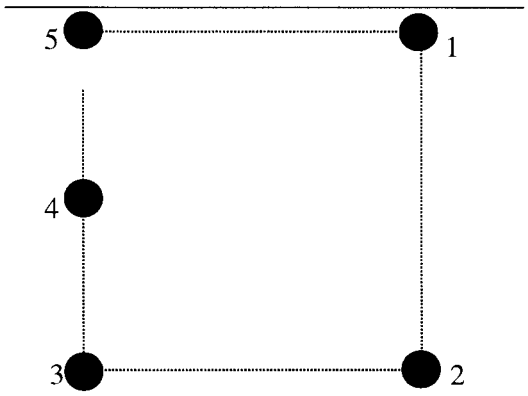

Points	Distance
1-2 / 1-5 / 2-3 / 2-5	120.0 mm
1-3 / 2-5	169.7 mm
1-4 / 2-4	134.2 mm

Figure 3. Test object to measure residual distortions. Distances between the points of the object are given in the table on the right.

room, by comparing the position of the spot with the point defined on the MR image. As proposed by other authors (3), we also use this system for stereo-localization of the needle, on the extremity of which are disposed five small infrared LEDs. The four cameras allow us to monitor the 3D area of possible positions of the extremity of the needle without imposing any constraints on surgeons regarding their placement in relation to the patient and the magnet. During the surgery performed while the patient is in the MR scanner, the system monitors in real time the position of inactive tip of the needle and measures trajectory deviations relating to the planned access path. In this manner, the surgeon is informed continuously about the position of the needle and overall errors in targeting via an LCD display placed in the magnet room. The system allows the accurate guidance of rigid surgical instruments such as biopsy needle or LITT optical fiber guides.

RESULTS

Measurements of the Distortions

The images were acquired with different MR sequences, as follows: spin echo (TR/TE 800/20 msec, bandwidth 49 Hz/pixel), turbo spin echo (TR/TE 800/24 msec, BW 65 Hz/pixel), fast low-angle shot (FLASH) 2D (TR/TE 800/9 msec, BW 78 Hz/pixel), and FISP (TR/TE 800/12 msec, BW 78 Hz/pixel), with contiguous 5-mm-thickness slices, matrix 256 × 256, and field of view (FOV) 250 × 250 mm^2. For each ball of the calibration phantom, we measured the distance between its actual position and its theoretical position. Figure 5 presents the results of the distortions vs. the distance from the magnet isocenter for each sequence.

These results allow us to define two distinct volumes. The first is a sphere of 150 mm radius in which the distortions remain moderate: it corresponds in fact to the homogeneity area (4 ppm) of the main magnetic field B_0 such as it is defined by the manufacturer. The second volume (the possible correction area), located between the previous sphere and a larger one (190 mm in radius), presents substantial but corrigible distortions. Beyond this second sphere, no correction is possible.

Evaluation of Residual Errors

The results obtained on the test object (Fig. 3) are given in Tables 1 and 2 and correspond a) to the case where the five markers are inside the B_0 homogeneity area; and b) to the case where markers 3, 4, and 5 are inside the possible correction area.

Determination of the Point of Entry and Needle Guidance

Tests were carried out to evaluate the robustness and precision of the indication by laser of the entry point. The residual error of the indication is on the order of 1 mm, negligible if we take into account the size of the laser spot (about 3 mm diameter). The time necessary to carry out the illumination is less than 5 seconds.

This system has been used to perform percutaneous bile duct drainage on an animal model (4). The accuracy of the performances obtained is better than 2 mm when indicating the needle entry point, and a terminal error better than 5 mm at 10 cm under the skin after biopsy needle placement when the software has guided the surgeon.

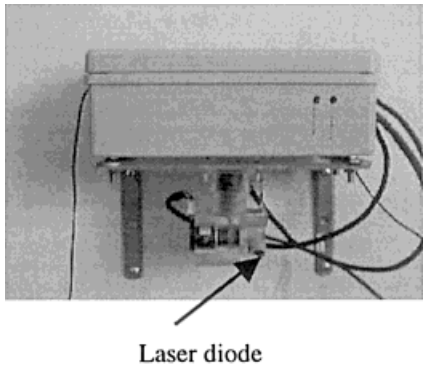

Figure 4. Laser pointer linked to the host computer by optical fibers to avoid MR artifacts.

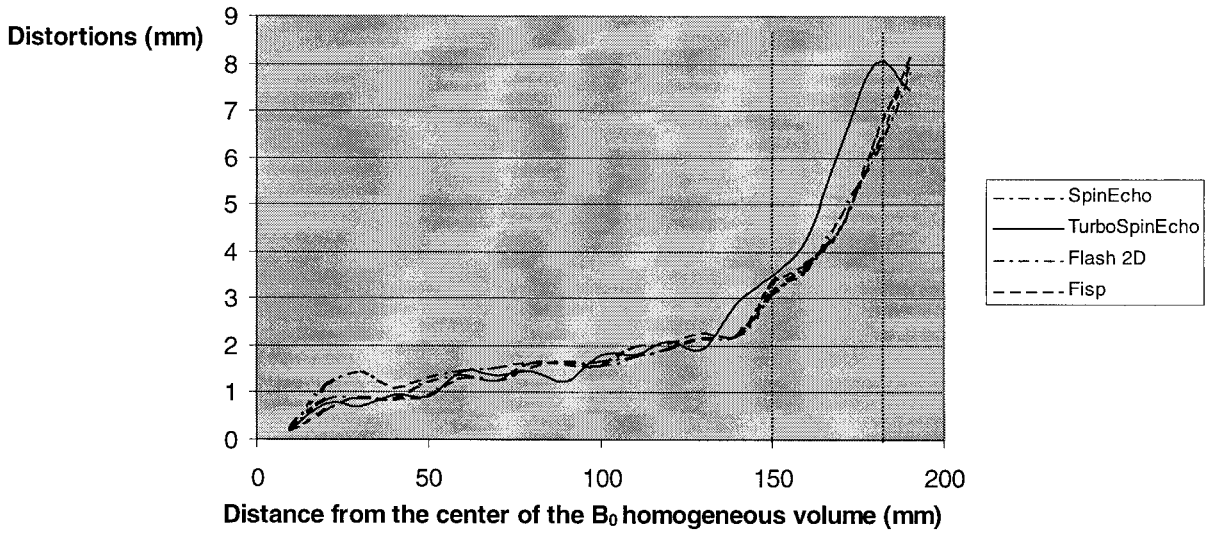

Figure 5. Image distortion vs. distance from the magnetic field isocenter, for the different MR sequences studied.

DISCUSSION

The measured image distortions were less than 3 mm inside the B_0 homogeneity volume, whatever the MR sequence used. This result shows that it is not necessary to correct the position of points located at a distance inferior to 150 mm from the center of the field. Nevertheless, the distortions increased up to 8 mm at 190 mm from the center. Thus, these corrections have to be corrected. Our results have shown that the proposed method makes it possible to define accurately the point of entry on a patient's skin.

The methods described in the literature model the deformations process or are based on information derived from additional images in order to correct the geometric deformations (1,5,6). Nevertheless, these methods can only be applied if the volume of interest lies within the B_0 homogeneity volume. During interventional MRI, the point of entry is often located outside this area. This can induce false 3D coordinates that can jeopardize the trajectory planning. The method described increases the planning accuracy by application of a correction when it is necessary.

To search for the entry point, the physician usually produces an artifact (eg, with a finger) on the patient's skin during nearly real-time image acquisition. However, the size of this artifact generally gives a great uncertainty of localization, which can induce major errors in trajectory planning. In fact, the trajectory of a needle can no longer be modified when it is inserted at a depth higher than approximately 2 cm. Under these conditions, the position of the entrance point and the direction of the needle must be given with a precision better than that which one wishes at the level of the target point. In the majority of the cases (biopsy, drainage, optical fiber guide, etc.) the targeting precision must be better than 5 mm. Our proposed method of laser pointing allows an accurate determination of the entry point (2 mm accuracy).

CONCLUSIONS

The realization of MR-guided procedures such as biopsy or installation of a guide requires precise placement of the instruments to reach the target. However, the success of these procedures could be compromised by geometric distortions of the images. This is why we have designed a method of correction of the 3D coordinates. Furthermore, we have developed a laser indication system to show the physician the point of entry on the skin. This technique makes it possible to avoid a system of markers and provides a visual indication of the entry point with a very good accuracy. In this way, it provides a quite practical solution to a problem that is quite common in interventional MRI procedures.

Table 1
Distance Errors (mm) Between Markers Before and After Distortion Correction When the Five Markers Are Inside the B_0 Homogeneity Volume

	Before correction	After correction			
		FISP	FLASH	SE	TSE
Mean error	1.2	0.3	0.4	0.3	0.9
SD	0.8	0.3	0.3	0.2	0.6
Maximum error	2.6	0.9	1.0	0.5	2.0

Table 2
Distance Errors (mm) Between Markers Before and After Distortion Correction When Markers 1 and 2 Are Inside the B_0 Homogeneity Volume*

	Before correction	After correction			
		FISP	FLASH	SE	TSE
Mean error	4.3	0.9	1.0	0.7	1.3
SD	1.5	0.7	0.7	0.6	1.1
Maximum error	6.7	1.9	2.6	2.0	3.4

*Markers 3, 4, and 5 are outside the homogeneity area but inside the possible correction volume.

ACKNOWLEDGMENTS

The authors thank L. Nicol from Siemens Medical System for constructive criticism and valuable comments.

REFERENCES

1. Michiels J, Bosmans H, Pelgrims P, et al. On the problem of geometric distortion in magnetic resonance images for stereotactic neurosurgery. Magn Reson Imaging 1994;12:749–765.
2. Boone JM, Seiber JA, Barret WA, Blood EA. Analysis and correction of imperfection in the image intensifier-TV-digitizer imaging chain. Med Phys 1991;18:236–242.
3. Silverman SG, Collick BD, Figueira MR, et al. Interactive MR-guided biopsy in an open-configuration MR imaging system. Radiology 1995;197:175–181.
4. Sergent G, Daanen V, Nicol L, et al. Percutaneous MR-guided bile duct drainage: first in vivo results. Proceedings of the 16th Annual ESMRMB meeting, Sevilla. MAGMA 1999;18:100.
5. Chang H., Fitzpatrick JM. A technique for accurate magnetic resonance imaging in the presence of field inhomogeneities. IEEE Trans Med Imaging 1992;11:319–329.
6. Sumanaweera TS, Glover GH, Hemler PF, et al. MR geometric distortion correction for improved frame-based stereotaxic target localization accuracy. Magn Reson Med 1995;34:106–113.